Several textural properties of compacted and cation-exchanged bentonite

G. Montes-Hernandez[a],*, J. Duplay[a], Y. Géraud[b], L. Martinez[c]

[a] *UMR 7566 UHP-CNRS, 54506 Vandoeuvre les-Nancy-Cedex, France*
[b] *UMR 7516 ULP-EOST, IPG 1, rue Blessig, F-67084 Strasbourg, France*
[c] *UMR G2R/7566, UHP Nancy I, BP 239, 54506 Vandoeuvre, France*

Abstract

One of the principal applications for bentonite is in drilling muds. Moreover it is widely used as a suspending and stabilizing agent, and as an adsorbent or clarifying agent, in many industries. Recently the bentonites have been proposed as engineered barriers for radioactive waste repository because these materials are supposed to build up a better impermeable zone around wastes by swelling. For these reasons, a textural characterization of bentonites in the laboratory is very important. The aim in this study was to estimate several textural properties of compacted and cation-exchanged bentonite by using Hg-porosimetry, N_2-adsorption, water vapour adsorption, scanning electron microscopy (SEM) observations and environmental scanning electron microscopy-digital images analysis measurements. For that, bulk samples were mechanically compressed at atmospheric conditions by using a uniaxial system at four different pressures (21, 35, 49, and 63 MPa) in order to obtain four physical densities. On the other hand, the bulk samples of bentonite were treated separately with four concentrated solutions (1N concentration) of sodium, potassium, magnesium and calcium chlorides in order to obtain a homoionic interlayer cation in the clay phase.

The results showed that the macro-porosity (porous size > 50 nm) and eventually the mesoporosity (porous size 2–50 nm) are affected by the uniaxial compaction. In this case, a transformation of the shape of the macro-pores network from tube to crack was observed. On the other hand, the swelling potential and water content are governed by the relative humidity and by the nature of interlayer cation.
© 2006 Elsevier Ltd. All rights reserved.

1. Introduction

The industrial and environmental uses of clays are expanding every year. One of the principal applications for bentonite is in drilling muds. Moreover it is widely used as a suspending and stabilizing agent, and as an adsorbent or clarifying agent in many industries because these materials are characterized by the fine particles with a high specific surface area and with a well adsorptive capacity of several chemical molecules and ions. Recently the swelling clays have been proposed as engineered barriers in the geological disposal systems for waste because these materials are supposed to build up a better impermeable zone around wastes by swelling [1–3]. Unfortunately, the swelling soils

are one of the nation's most prevalent causes of damage to buildings and construction. The losses include severe structural damage, cracked driveways, sidewalks and basement floors, heaving of roads and highway structures, condemnation of buildings, and disruption of pipelines and sewer lines [4,5]. For these reasons, the estimation of textural properties of clays in the laboratory is very important. Many analytical tools are available for the estimation of textural properties of clays. In the current study, several textural properties of compacted and cation-exchanged bentonite were estimated by using Hg-porosimetry, N_2-adsorption, water vapour adsorption, scanning electron microscopy (SEM) and environmental scanning electron microscopy (ESEM) observations and environmental scanning electron microscopy-digital images analysis (ESEM-DIA) measurements. For that, four bulk samples were mechanically compressed at atmospheric conditions by using a uniaxial system (limit of upward

---

*Corresponding author. Tel.: 00 333 8368 4752.
E-mail addresses: german.montes@g2r.uhp-nancy.fr,
german_montes@hotmail.com (G. Montes-Hernandez).

thrust = 50kN) at different pressures (21, 35, 49, and 63 MPa) in order to obtain four physical densities. These samples were labeled as MX80-21 MPa, MX80-35 MPa, MX80-49 MPa, MX80-63 MPa. On the other hand, the bulk samples of bentonite were treated separately with four concentrated solutions (1N concentration) of sodium, potassium, magnesium and calcium chlorides, all salts with the same ionic force ($I = 2$). This treatment was made three times with constant agitation for 1 h. Then, the clay was washed three or four times with distilled water until the $AgNO_3$ test for chloride was negative. The scanning transmission electron microcopy (STEM) and ICP-AES analyses were used to notice the homoionic interlayer cation in the clay phase. In this case, the samples were labeled as Na-bentonite, K-bentonite, Mg-bentonite and Ca-bentonite.

2. Material and methods

2.1. Bentonite characterization

XRD analysis was carried out directly on raw-bentonite (minerals identification) and oriented clay fraction "$< 2\,\mu m$" (identification of clay family). A comparative analysis with the X-ray diffractogramm corresponding to clay mineral permitted to identify the quartz and the montmorillonite as the main mineral phases. In addition the X-ray diffractogramm corresponding to the clay fraction shows that the clay family corresponds to a typical smectite "montmorillonite," since the ethylene glycol test shows a shift of the 12 Å peak up to 17.14 Å. The 12 Å peak is closed up to 9.66 Å when the sample is dried at 490 °C.

The clay fraction morphology and chemical composition were studied by means of STEM and ICP-AES. STEM analysis shows folded particles and turbostratic sheets stacking. The average chemical composition obtained by this method permitted a structural formula estimation:

$$(Si_{3.99}Al_{0.01})(Al_{1.5413}Mg_{0.2448}Fe(III)_{0.1893})Na_{0.2186}Ca_{0.057}O_{10}(OH)_2.$$
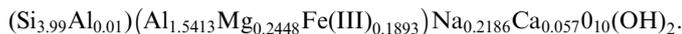
This structural formula corresponds to a low charge montmorillonite with mixed "Na–Ca" filling interlayer.

The complete characterization to estimate the mineral composition of MX80 bentonite was achieved by different French laboratories (LEM-CREGU). These laboratories concluded that the bentonite contains Na/Ca-montmorillonite (80%), quartz (6%), K-feldspars (2%), plagioclases (4%), carbonates (4%), mica (3%) and other minerals (1%) [6].

2.2. Samples preparation

2.2.1. Uniaxial compaction

Four bulk samples were mechanically compressed by a uniaxial system (limit of upward thrust = 50kN) at different pressures (21, 35, 49 and 63 MPa) in order to obtain four physical densities. The displacement speed during mechanical compaction was kept constant at 5 μm/s on all the samples. The mechanical compaction was realized at atmospheric conditions (room temperature = 20 °C and atmospheric pressure about $1 \times 10^5 Pa$). In these conditions, the amount of adsorbed water of the bulk samples was estimated at 0.1151 kg/kg of dry clay, i.e. the initial water content of the clay was 11.5%. However, the water content of compacted samples at same atmospheric conditions was estimated between 10% and 11%. In order to keep constant the hydration state of compacted samples, they were stoked in the plastic desiccators (2 l). Here the water activity of air "into the plastic desiccators" and surrounding samples contained in the glass jar was controlled at 0.55 with an oversaturated salt solution ($Na_2Cr_2O_7$).

It is obvious that each mechanical pressure induced a physical density. Here the physical densities were manually estimated on the cylindrical pastilles. These measures were realized at atmospheric conditions, which means that the samples were partially hydrated (10–11%). The values estimated are summarized in the Table 1.

The total samples used in this paper were labeled as MX80-21 MPa, MX80-35 MPa, MX80-49 MPa and MX80-63 MPa.

2.2.2. Cation exchange

On the other hand, the bulk samples of MX80 bentonite were treated separately with four concentrated solutions (1-N concentration) of sodium, calcium, magnessium, and potassium chlorides. All salts have the same ionic force ($I = 2$).

Twenty grams of MX80 bentonite were dispersed into 1 L of salt solution (1N) at 60 °C. This suspension was vigorously stirred with magnetic agitation for 1 h at 60 °C. Then, the cation-exchanged clay was separated by centrifugation (15 min at 13000 rpm) and decanting the supernatant solutions. This process was repeated three times. The cation-exchanged bentonite was then washed three to four times with distilled water until the $AgNO_3$ test for chloride is negative. The cation-exchanged bentonite was subsequently dried for 48 h at 60 °C and finally ground for 2 min [7]. The scanning transmission electron microcopy

Table 1
Physical characteristics of MX80 bentonite submitted to different mechanical compaction

Sample label	Confining pressure [MPa]	Physical density [kg/m³]	S_{BET} [m²/kg]	$W\ a_w = 0.95$ [kg/kg$_{dry\ clay}$]
MX80-21 Mpa	21	1820	21230	0.2822
MX80-35 Mpa	35	1950	23180	0.2895
MX80-49 Mpa	49	2030	22790	0.2896
MX80-63 MPa	63	2080	20370	0.2910

S_{BET}: specific surface area (BET method), W: maximal amount of adsorbed water.

(STEM) and ICP-AES analyses were used to notice the homoionic interlayer cation in the clay phase. In this case, the samples were labeled as Na-bentonite, K-bentonite, Mg-bentonite and Ca-bentonite.

The N_2-adsorption [8,9], SEM and ESEM observations [7,10–12], Hg-Porosimetry [13], isothermal adsorption of water vapour [7], and ESEM-DIA measurements [7,14] were carried out in order to estimate several textural properties of compacted and cation-exchanged bentonite. The methodology for these methods is not explained in this paper.

3. Results and discussion

3.1. Compacted bentonite

3.1.1. Hg-porosimetry and SEM observations

The mercury injection porosimetry shows that only the macro-porosity (porous size > 50 nm) and eventually meso-porosity (porous size 2–50 nm) are affected by the mechanical compaction (see Fig. 1a and b). For example, the Fig. 1a shows clearly how the pore size distribution is displacing with mechanical compaction intensity. Indeed the total porosity decreases when the physical density increases (Fig. 1b). These results are coherent with literature.

SEM observations confirm that the mechanical pressures induce modifications of the inter-aggregate's porous (porous size > 5 μm). The macro-pores of the inter-aggregate network presents a variation of form, from tubular at moderate pressure of compactions to a system of cracks for high pressure of compaction (see Fig. 2).

3.1.2. Adsorption isotherms of water vapour and adsorption isotherms of N_2

Experimental water adsorption data were fitted by the D'Arcy and Watt equation. This equation considers the monolayer (Langmuir) and multilayer (BET) adsorption [15]. The equation used in terms of water activity "a_w" was

$$W = \frac{w_1 c_1 a_w}{1 + c_1 a_w} + p a_w + \frac{w_M c_M a_w}{1 - c_M}, \tag{1}$$

where W is the amount of water adsorbed, w_1 and w_M are the densities of the primary and multilayer adsorption sites, respectively, c_1 and c_M are the interaction parameters related to the heat of adsorption on the primary adsorption sites and in the multilayer, respectively, and p is a constant included in the linear form of the adsorption isotherm.

A computer program (SigmaPlot2000) based on the non-linear least-squares analysis was used for fitting the equation to the water adsorption data. This fitting was only used to characterize the shape of adsorption–desorption isotherms.

The adsorption isotherms of water vapour at 23 °C are shown in the Fig. 3. The shapes of these isotherms seem to correspond to type III of the modern IUPAC classification of isotherms [16]. That is, the isotherms with small solid-

(a)

(b)
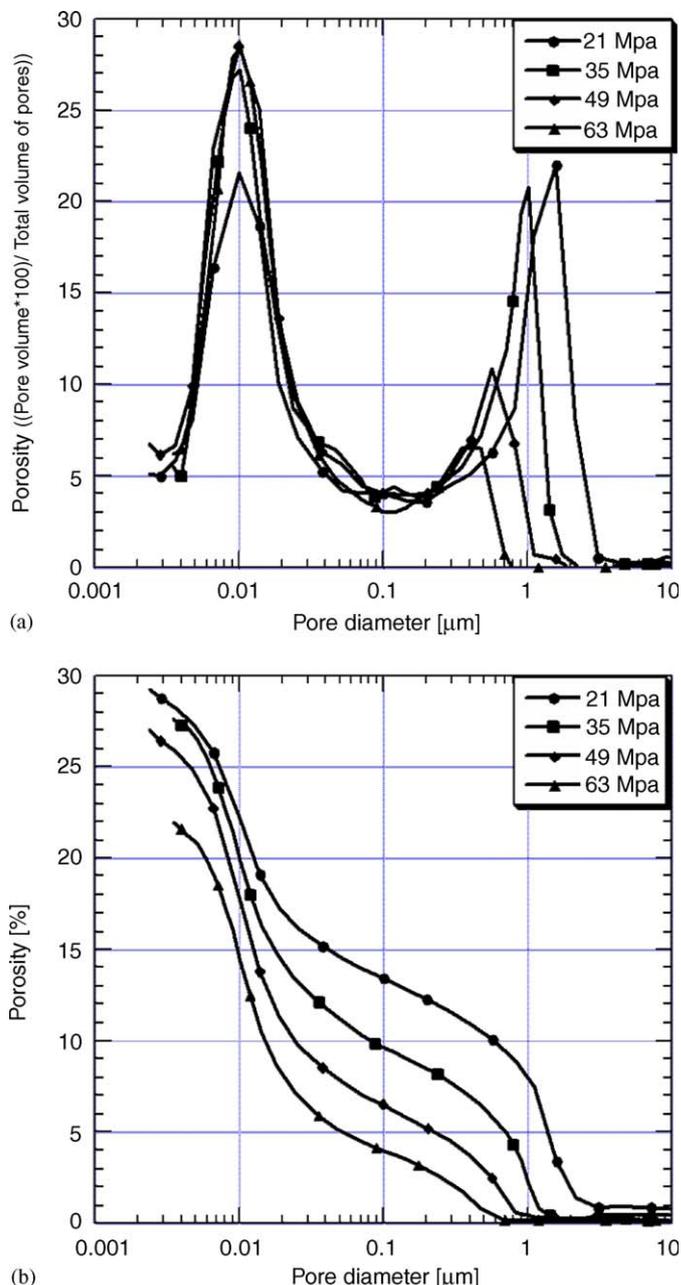
Fig. 1. (a) Pores size distribution to different confining pressure. (b) Total porosity behaviour to different confining pressure.

fluid interaction at low water activities (< 0.5). In contrast, a very high potential of water adsorption was observed at high water activities (> 0.5). This may correspond to the formation of water multilayer around the interlayer cation and also to the water capillary condensation.

It is necessary to mention that isotherms III in the IUPAC classification were proposed to describe macro-porous systems. In general, that is not the case for clay minerals. In addition, the interlayer cations play an important role in the water adsorption and swelling. This situation makes a complex mechanism for water adsorption as a function of water activity. Finally, the adsorption
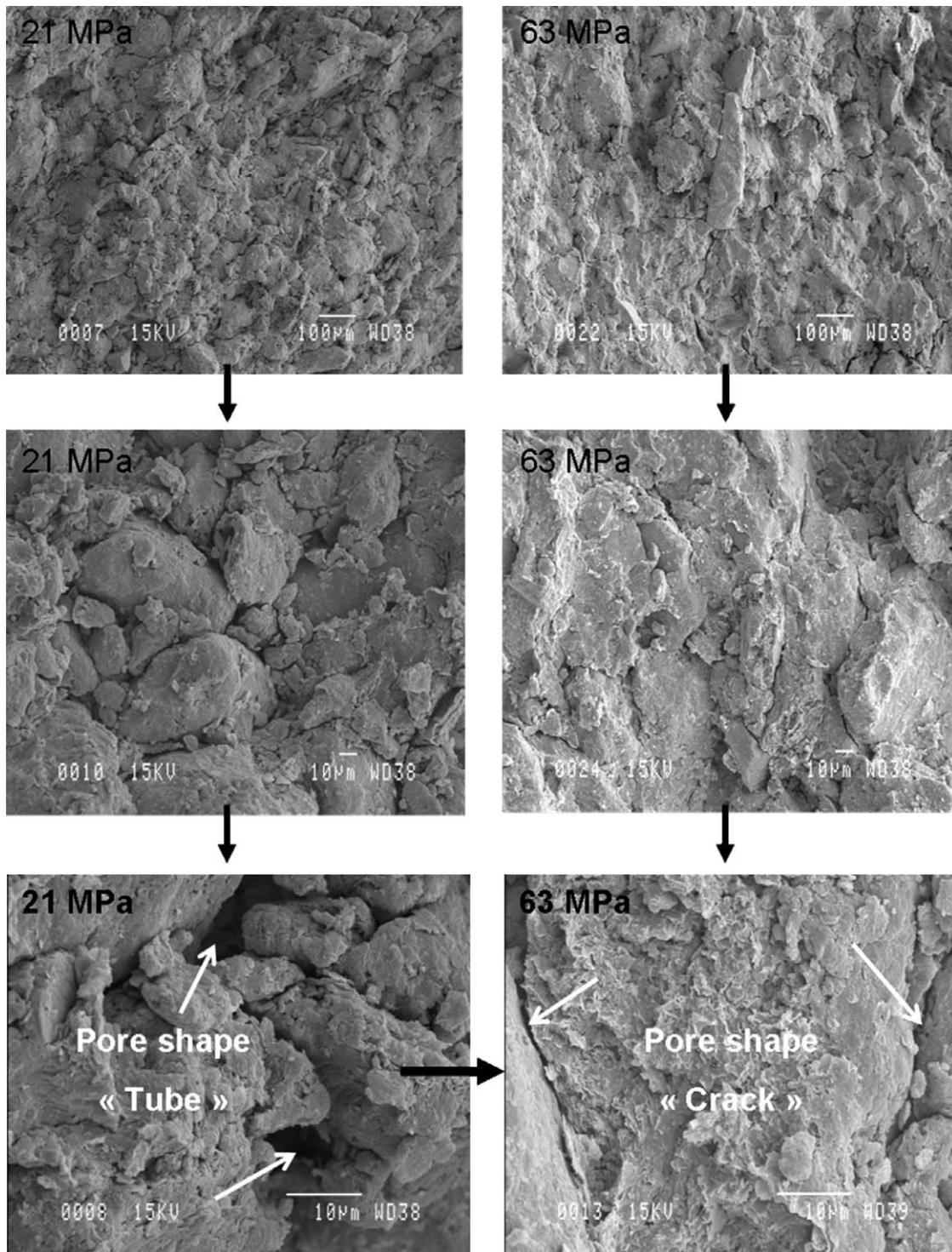
Fig. 2. SEM micrographs. Porous network comparison between a moderate compaction pressure (21 MPa) and a high compaction pressure (63 MPa) of MX80 bentonite.

isotherms of water vapour (Fig. 3) shows that the amount of adsorbed water as a function of water activity is not affected with mechanical compaction. In fact, the four water adsorption isotherms are very similar. This assumption is confirmed by N_2 adsorption; in this case the isotherms are also very similar (Fig. 4). These results allow of supposing that the micro-porosity is insignificantly affected with the mechanical compaction. In fact, the amount of adsorbed water and adsorbed volume of N_2 of compacted samples is almost constant as a function of water activity or as a function of relative pressure, respectively.
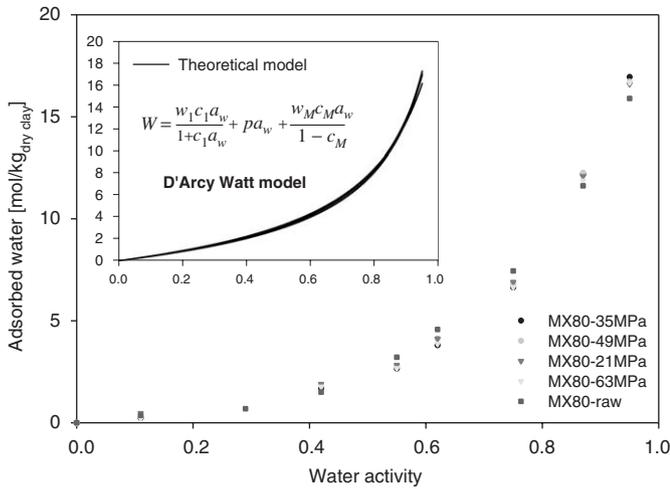
Fig. 3. Adsorption isotherms of water vapour. MX80 bentonite compressed to four confining pressures. Experimental data fitted by D'Arcy Watt equation.
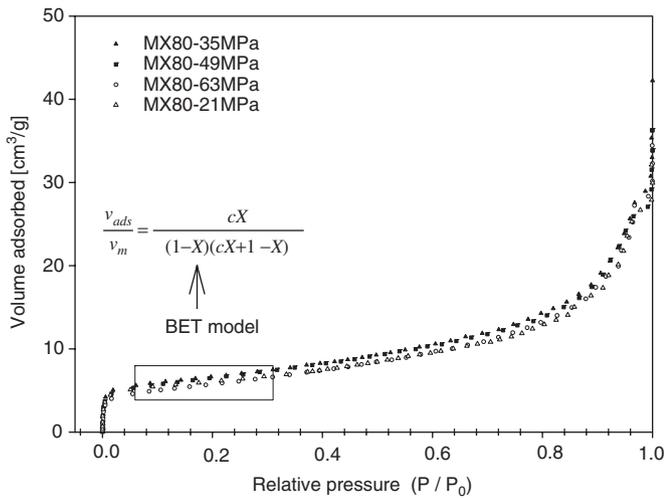
Fig. 4. N_2-adsorption isotherms for compacted bentonite. Specific surface area estimated by BET equation.

3.2. Raw and cation-exchanged bentonite

By coupling ESEM with DIA it was possible to identify three stages for the kinetics of the swelling at the "aggregate scale" (Fig. 5). The first stage is very difficult to model, because of the random arrangement of the particles in the initial water adsorption. In general this stage is characterized by a non-swelling feature and sometimes by an aggregate contraction. The second stage presents a high swelling during first minute, after which the swelling decreases gradually up to an asymptotic maximum of time. This stage may be modeled by an exponential equation. The third stage called "aggregate water over-saturation" is only presented at a critical relative humidity comprised between 80 and 95%. The first and second stages were also identified by the mechanical methods for other expansive clays (for more information to consult [14,17]).
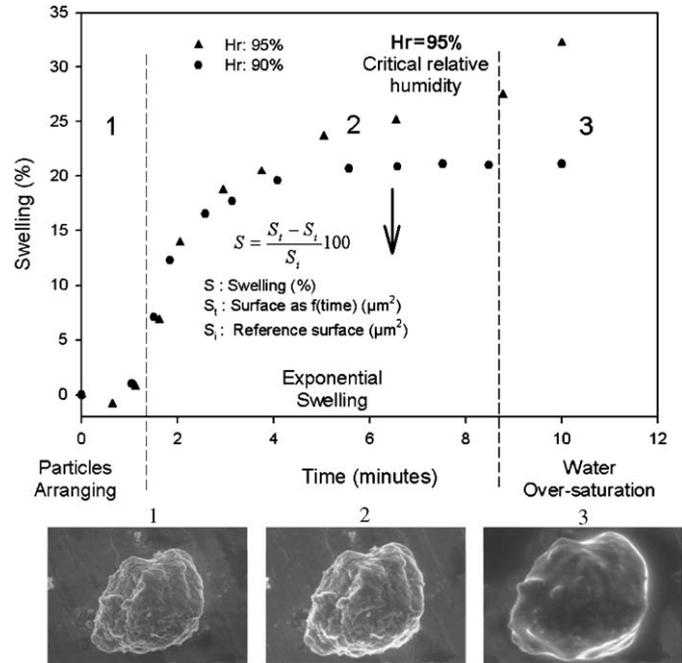
Fig. 5. Swelling kinetics of raw bentonite aggregate scale using ESEM-DIA coupling [14].
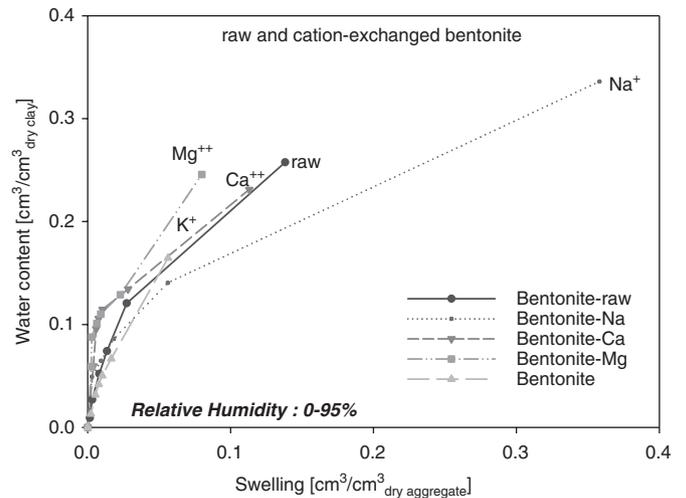
Fig. 6. Water content and swelling potential correlation for raw and cation-exchanged bentonite. The swelling potential was considered as equidimensional to aggregate scale.

The swelling potential and water content of bentonites are dependent on the nature of interlayer cation in the clay phase. In the current study, it was observed that Na-exchanged bentonite presents an excellent capacity to swell and to adsorb water, while the Ca-exchanged, Mg-exchanged and K-exchanged bentonites swell and adsorb water less significantly at high relative humidities ($> 50\%$). The raw bentonite displays intermediate swelling potential and water content, because of the montmorillonite, which presents both Na and Ca in the interlayer (see Fig. 6). Finally, a nonlinear correlation was observed between

swelling potential and water content. But, this basic approach must be considered with care since the measurements of the amount of adsorbed water and swelling potential were estimated separately by different analytical methods with different scales.

4. Conclusion

Hg-porosimetry shows that only the macro- porosity (porous size > 50 nm) and eventually the meso- porosity (porous size between 2 and 50 nm) are affected by the mechanical compaction. In fact, the total porosity decreases when the mechanical compaction increases. In this case, SEM observations show a transformation of the shape of the macro-pores network from tube to crack. On the other hand, adsorption isotherms of N_2 and adsorption isotherms of water vapour show that microporosity remains practically intact.

The coupling ESEM with DIA is a powerful method to estimate the swelling–shrinkage potential of expansive clays. The main advantage of this method is the rapidity with which one obtains the qualitative and quantitative results. However this method allows only the estimation of the free swelling/shrinkage potential in the sample chamber. In situ observations with ESEM allowed to identify three steps for the swelling kinetic: (1) particles arrangement; (2) exponential swelling; (3) water over-saturation.

Finally, the swelling potential and water content are governed by the relative humidity and by the nature of interlayer cation. For example, globally the Na-exchanged bentonite presents an excellent capacity to swell and to adsorb while the Ca-exchanged, Mg-exchanged bentonite and K-exchanged bentonites swell and adsorb less significantly at high relative humidities (> 0.5).

Acknowledgements

References

[1] H.H. Murray, Traditional and new applications for kaolin, smectite, and palygorskite: a general overview, Appl. Clay Sci. 17 (2000) 207–221.

[2] R. Pusch, Use of bentonite for isolation of radioactive waste products, Clay Miner 27 (1992) 353–361.

[3] D. Koch, Bentonites as a basic material for technical base liners and site encapsulation cut-off walls, Appl. Clay Sci. 21 (2002) 1–11.

[4] A.A. Al-Rawas, The factors controlling the expansive nature of the soils and rocks in northern Oman, Eng. Geol. 53 (1999) 327–350.

[5] A.A. Al-Rawas, G. Ingeborg, A. McGown, Geological and engineering characteristics of expansive soils and rocks in northern Oman, Eng. Geol. 50 (1998) 267–281.

[6] E. Sauzeat, D. Guillaume, A. Neaman, J. Dubessy, M. François, C. Pfeiffert, M. Pelletier, R. Ruch, O. Barres, J. Yvon, F. Villéras, M. et Cathelineau, Caractérisation minéralogique, cristallochimique et texturale de l'argile MX80. Rapport ANDRA No. CRP0ENG 01-001, (2001), 82p.

[7] G. Montes-H, J. Duplay, L. Martinez, Y. Geraud, B. Rousset-Tournier, Influence of interlayer cations on the water sorption and swelling-shrinkage of MX80 bentonite, Appl. Clay Sci. 23 (2003) 309–321.

[8] A. Neaman, M. Pelletier, F. Villieras, The effects of exchanged cations, compression, heating and hydration on textural properties of bulk bentonite and its corresponding purified montmorillonite, Appl. Clay Sci. 22 (2003) 153–168.

[9] F. Villiéras, R. Leboda, B. Charmas, F. Bardot, G. Gérard, W. Rudzinski, High resolution argon and nitrogen adsorption assessment of the surface heterogeneity of carbosils, Carbon 36 (10) (1998) 1501–1510.

[10] G. Montes-H, Etude expérimentale de la sorption d'eau et du gonflement des argiles par microscopie électronique à balayage environnementale (ESEM) et analyse digitale d'images, Ph.D. Thesis, Louis Pasteur University, Strasbourg I, France, 151p, (2002).

[11] H.G. Montes, J. Duplay, L. Martinez, S. Escoffier, D. Rousset, Structural modification of Callovo-Oxfordian argillite under hydration/dehydration conditions, Appl. Clay Sci. 25 (2004) 187–194.

[12] G. Montes-H, Y. Géraud, J. Duplay, ESEM observations of compacted bentonite submitted to hydration/dehydration conditions, Colloids and Surfaces A: Physicochem. Eng. Aspects 262 (2005) 14–22.

[13] Y. Géraud, J-M. Caron, P. Faure, Porosity network of a ductile shear zone, J. Struct. Geol. 17 (12) (1995) 1757–1769.

[14] G. Montes-H, Swelling-shrinkage measurements of bentonite using coupled environmental scanning electron microscopy and digital image analysis, Journal of Coll. Interface Sci. 284 (2005) 271–277.

[15] M. Sychev, R. Prohod'ko, A. Stepanenko, M. Rozwadowski, V.H.J. San de Beer, R.A. Van Sarten, Characterization of the microporosity of chromia- and titania-pillared montmorillonites differing in pillar density : II Adsorption of benzene and water, Micropor. Mesopor. Mater. 47 (2001) 311–321.

[16] G. Aranovich, M.D. Donohue, Adsorption hysteresis in porous solids, J. Colloid Interface Sci. 205 (1998) 121–130.

[17] G. Montes-H, J. Duplay, L. Martinez, C. Mendoza, Swelling-Shrinkage kinetics of MX80 bentonite, Appl. Clay Sci. 22 (2003) 279–293.